Published in final edited form as:

Nat Immunol. 2016 May ; 17(5): 538–544. doi:10.1038/ni.3417.

Acidic chitinase primes the protective immune response to gastrointestinal nematodes

Kevin M Vannella[1], **Thirumalai R Ramalingam**[1], **Kevin M Hart**[1], **Rafael de Queiroz Prado**[1], **Joshua Sciurba**[1], **Luke Barron**[1], **Lee A Borthwick**[1,2], **Allen D Smith**[3], **Margaret Mentink-Kane**[1], **Sandra White**[1], **Robert W Thompson**[1], **Allen W Cheever**[1], **Kevin Bock**[4], **Ian Moore**[4], **Lori J Fitz**[5], **Joseph F Urban Jr**[3], and **Thomas A Wynn**[1]

[1]Program in Tissue Immunity and Repair, Laboratory of Parasitic Diseases, National Institute of Allergy and Infectious Diseases, National Institutes of Health, Bethesda, Maryland, USA

[2]Tissue Fibrosis and Repair Group, Institute of Cellular Medicine, Newcastle University, Newcastle upon Tyne, UK

[3]United States Department of Agriculture, Agricultural Research Service, Beltsville Human Nutrition Center, Beltsville, Maryland, USA

[4]Infectious Disease Pathogenesis Section, National Institute of Allergy and Infectious Diseases, National Institutes of Health, Rockville, Maryland, USA

[5]Inflammation and Immunity, Pfizer Worldwide R&D, Cambridge, Massachusetts, USA

Abstract

Acidic mammalian chitinase (AMCase) is known to be induced by allergens and helminths, yet its role in immunity is unclear. Using AMCase-deficient mice, we show that AMCase deficiency reduced the number of group 2 innate lymphoid cells during allergen challenge but was not required for establishment of type 2 inflammation in the lung in response to allergens or helminths. In contrast, AMCase-deficient mice showed a profound defect in type 2 immunity following infection with the chitin-containing gastrointestinal nematodes *Nippostrongylus brasiliensis* and *Heligmosomoides polygyrus bakeri*. The impaired immunity was associated with reduced mucus production and decreased intestinal expression of the signature type 2 response genes *Il13*, *Chil3*, *Retnlb,* and *Clca1*. CD103^{+} dendritic cells, which regulate T cell homing, were also reduced in mesenteric lymph nodes of infected AMCase-deficient mice. Thus, AMCase

Correspondence should be addressed to T.A.W. (twynn@niaid.nih.gov).

Accession codes. NCBI GenBank: *Rplp2*, NM_026020; *Chia1*, NM_023186; *Il4*, NM_021283; *Il13*, NM_008355; *Chil3*, NM_009892; *Relnlb*, NM_023881; *Retnla*, NM_020509; *Clca1*, NM_017474; *Il5*, NM_010558; *Il25*, NM_080729; *Il33*, NM_001164724; *Tslp*, NM_021367; *Mrc1*, NM_008625; *Chit1*, NM_001284525.

Note: Any Supplementary Information and Source Data files are available in the online version of the paper.

AUTHOR CONTRIBUTIONS

K.M.V., T.R.R. and T.A.W. conceived and designed the experiments; K.M.V., A.D.S., K.M.H., L.A.B., R.W.T., S.W., J.F.U., R.d.Q.P. and J.S. performed the experiments; I.M. and K.B. performed immunofluorescence techniques; K.M.V., T.R.R., A.D.S., A.W.C., L.B., L.A.B., M.M.-K., T.A.W., J.F.U. and R.d.Q.P. analyzed the data; A.D.S., A.W.C., I.M., J.F.U. and L.J.F. contributed reagents; K.M.V., T.R.R. and T.A.W. wrote the paper.

COMPETING FINANCIAL INTERESTS

The authors declare no competing financial interests.

functions as a critical initiator of protective type 2 responses to intestinal nematodes but is largely dispensable for allergic responses in the lung.

Chitin is the second most abundant polymer in nature, found as a structural component in fungi[1], arthropods[2], and parasitic nematodes[3,4]. Mammals do not synthesize chitin, but they express two known enzymes that digest chitin: acidic mammalian chitinase (AMCase)[5] and chitotriosidase[6]. It is known that AMCase is expressed in the lung and the gastrointestinal tract of humans and mice, and that its activity is markedly increased in epithelial cells and macrophages in response to the type 2 cytokines IL-4 and IL-13, yet its role in type 2 inflammation and immunity remains unclear[7–9]. Most studies investigating AMCase function have focused on its role in allergic lung disease. Mice congenitally lacking AMCase (AMCase-deficient) demonstrated little to no role for the enzyme in acute models of house-dust-mite- or ovalbumin (OVA)-induced allergy in the lung[10]. These findings contrasted with those of another published study in which neutralizing AMCase activity with allosamidin or with a monoclonal antibody resulted in marked diminution of IL-13-driven allergic inflammation, suggesting that the enzyme might represent an attractive therapeutic target in allergic asthma[7]. Still, additional reports have proposed that AMCase has a protective role. One showed that the type 2 inflammatory response following chitin challenge was ameliorated in mice overexpressing AMCase[8], and another observed increased allergic lung disease in mice specifically lacking AMCase enzymatic activity[11]. The contrasting functional implications of AMCase highlighted in these studies have yet to be fully reconciled. Further, allergic inflammation recapitulates the prototypic type 2 response seen after helminth infection[12], but, surprisingly, despite the discovery that AMCase is highly expressed after exposure to helminths[13], it has remained unknown whether the enzyme has any role in the host immune response to these important human pathogens.

In this study, we used AMCase-deficient mice as a means to dissect the role of the enzyme in several models of helminth infection and type 2 cytokine–driven airway inflammation. We show that although AMCase activity is largely dispensable in the development of allergic airway disease, the enzyme plays a critical role in the development of type 2 immunity to the gastrointestinal nematodes *N. brasiliensis* and *H. p. bakeri*.

RESULTS

Fewer ILCs but normal allergy in AMCase-deficient mice

Our initial studies were focused on reconciling the conflicting observations generated in models of allergic lung inflammation. We postulated that the higher doses of allergen used in a previously published study (involving intranasal sensitization and challenges with 100 μg house dust mite allergen, HDM) could have masked a role for AMCase, thus accounting for the different observations described above[10,11]. Accordingly, we administered a low-dose allergen time course (intranasal sensitization and challenges with 25 μg and 5 μg HDM, respectively) to AMCase-deficient mice. A day after the last of four challenge doses, we found that the low doses of allergen increased the lung tissue expression of *Chia1*, the gene encoding AMCase in wild-type mice (Fig. 1a), but that both wild-type and AMCase-

deficient mice exhibited similar pulmonary inflammatory pathology (Fig. 1b). In the tissue, AMCase abrogation did not have a significant impact on leukocyte or eosinophil accumulation or on gene expression of the type 2 cytokines IL-5 and IL-13 (Fig. 1c). At this time point, genes for type 2 initiators IL-33 and TSLP and for the alternative activation markers Relmα and Mrc1 also were expressed at similar levels in both groups of mice. Moreover, AMCase deficiency did not alter type 2 inflammation in the airways (Fig. 1d). Confirming that these observations were not unique to HDM, we found similar results with papain, a nonchitinous allergen (Supplementary Fig. 1). We were able to detect gene expression of chitotriosidase in naive and allergic lung tissue, although it was not elevated during the allergic response (Fig. 1e). Inquiries into whether chitotriosidase has a critical function in lung allergy and into the differences between mice with enzymatically inactive AMCase and mice deficient in the entire AMCase protein remain to be performed.

Although AMCase ablation had no effect on the development of allergic disease, we found evidence that the innate type 2 response was reduced in AMCase-deficient mice. Following only sensitization with HDM, fewer total leukocytes and fewer IL-5^{+}IL-13^{+} type 2 innate lymphoid cells (ILC2 cells) were observed in the lungs of AMCase-deficient mice (Fig. 1f). In addition, fewer ILCs expressed GATA-3 protein, a transcription factor critically required for the development of ILC2s[14]. Although AMCase-deficient mice ultimately overcame this defect at later time points, these data suggest, for the first time, an important role for AMCase in type 2 immune priming upstream of ILCs. Whether this early immune priming defect explains why polymorphisms of AMCase are associated with airway allergy requires further investigation[15]. Our data indicate that AMCase plays a role in the initiation of type 2 immune responses but is not required for the establishment of type 2 allergic inflammation in the lung.

We also extended our studies to a chronic model of HDM-induced allergy over 6 weeks, and here, too, found little to no role for AMCase (Fig. 2). These data bolster the conclusions of previous studies showing that AMCase ablation does not have a significant effect on allergic airway pathology. They also support other reports that chitotriosidase is the primary active chitinase in the lung[16,17].

Lung granulomas form without AMCase

Next, we investigated whether AMCase is required for the type 2 response to helminth parasites known to increase AMCase expression[13,18]. We began by using a *Schistosoma mansoni* parasite egg–induced pulmonary granuloma model, in which intravenously injected eggs that become trapped in the pulmonary vasculature trigger endothelial cell damage, potent type 2 inflammation, and IL-4- plus IL-13-dependent granuloma formation. *S. mansoni* egg exposure led to an IL-13-dependent upregulation of *Chia1*, which was more robust than that induced by HDM (Fig. 3a). Immunofluorescence staining localized the protein expression predominantly to bronchial epithelial cells (Fig. 3b). Despite the marked induction of AMCase in wild-type lungs, granuloma formation (Fig. 3c), fibrosis (Fig. 3d), mucus production (Fig. 3e), granulomatous eosinophil accumulation (Fig. 3f), and total leukocyte accumulation in bronchoalveolar lavage fluid (BALF) (Fig. 3g) were unimpaired in AMCase-deficient mice, demonstrating AMCase is not categorically required to mount

wild-type antiparasite responses. Likewise, intratracheal delivery of schistosome egg antigen (SEA) upregulated *Chia1* in the lung, but the type 2 response was unaffected in AMCase-deficient mice, suggesting that the lack of phenotypic alteration was not due to the route of antigen delivery (intravascular versus epithelial exposure, Supplementary Fig. 2). Instead, the findings support the lung allergy studies that concluded AMCase does not have important regulatory activity in the lung.

AMCase is critical for protection against *N. brasiliensis*

AMCase is highly expressed in the gastrointestinal tract (GI), but it was unknown whether AMCase is important for the development of immunity to gastrointestinal parasites that elicit a type 2–polarized protective immune response. GI roundworms or nematodes, which, unlike the flatworm trematode *S. mansoni*, are known to contain chitin in their mouthparts, larval sheaths, and eggshells[3,4], infect over 2 billion people, contributing to substantial morbidity and mortality worldwide[19]. We sought to understand the role of AMCase in host protection using the rodent nematode *N. brasiliensis*, which has been used extensively to study and model the immunobiology of human hookworm infestation[20]. In the mouse model, after subcutaneous injection of infectious larvae, *N. brasiliensis* traverses the lung within 1–2 d before migrating up the trachea and entering the GI tract, where larvae mature into egg-laying adults. Wild-type mice successfully expel the worms by around 10–14 d after initial infection[21]. We enumerated the number of *N. brasiliensis* larvae in the wild-type or AMCase-deficient guts 5, 8, 10, and 14 d after infection. The number of worms that traversed the lungs and took residence in the gut on day 5 did not differ between AMCase-sufficient and -deficient mice (Fig. 4a). Although wild-type mice expelled the worms nearly completely by day 10, as expected, AMCase-deficient mice harbored significantly more worms in the intestine, and most did not fully clear the infection even by day 14 (Fig. 4a). The impaired host response resulting from AMCase deficiency was also characterized by a marked increase in the number of parasite eggs in the feces of infected AMCase-deficient mice (Fig. 4b).

To investigate the reasons for the impairment in host defense, we harvested lung, stomach, and intestinal tissue 8 d after infection, the peak of expulsion in wild-type mice. In the lung, *Chia1* expression was upregulated as previously described[8], but *Il13* and the majority of known effector molecules tested were expressed comparably in wild-type and AMCase-deficient mice (Supplementary Fig. 3). Only *Chil3* (the gene encoding the chitinase-like protein, Ym1) expression was significantly impaired ($P < 0.05$) in AMCase-deficient lungs even a few days after worm passage—which is notable because Ym1 induces IL-17 and neutrophilic inflammation in the lung that has been postulated to compromise the fitness of *N. brasiliensis* larvae[22]. Reminiscent of the original description of AMCase[5], *Chia1* expression in the intestines was undetectable, but it was higher, by at least one order of magnitude, in the stomach than in the lung (Fig. 4c). In contrast to the lung, where expression held steady, intestines of AMCase-deficient mice had greatly diminished expression of chitotriosidase during *N. brasiliensis* infection (Fig. 4d). The gene-expression profile in the intestine also correlated with a broadly impaired host response to *N. brasiliensis,* with AMCase-deficient mice exhibiting markedly reduced expression of *Il13* and several key downstream type 2 effector genes (Fig. 4d). *Il13* expression was reduced by

more than 50%, and *Chil3* expression, which is upregulated over 2,000-fold in infected wild-type intestine, was nearly completely abrogated, approaching the levels found in uninfected mice. Perhaps most notably, AMCase was necessary for normal expression of *Retnlb*, the gene encoding another mediator previously shown to be essential for normal nematode expulsion[21]. Expression of *Clca1*, which encodes a chloride channel (Gob5) involved in mucus production[23], was also reduced. This defect likely explains the diminished production of mucus from intestinal goblet cells, which is also critical to the development of protective immunity[24] (Fig. 4e). Accordingly, the kinetics of *N. brasiliensis* clearance in the AMCase-deficient mice were similar to those seen in past studies of mice deficient in IL-13 signaling[25,26]. Collectively, our data show that AMCase is necessary for mice to mount normal type 2 immunity against *N. brasiliensis*.

Impaired immunity against *H. p. bakeri*

Lastly, because AMCase is expressed in the lung, we sought to explore whether the defective type 2 response in AMCase-deficient mice after *N. brasiliensis* infection was also observed after primary and secondary infection with *H. p. bakeri*, a rodent nematode that is acquired orally, is restricted to the GI tract, and does not migrate through the lungs. Also, in contrast to the *N. brasiliensis* model, wild-type mice do not clear primary infection with *H. p. bakeri,* but upon antihelminthic treatment, subsequent infections are successfully eliminated—making this an ideal model in which to explore the role of AMCase in the development and maintenance of secondary immunity. Wild-type mice showed a marked increase in *Chia1* mRNA expression in the stomach after infection that was absent in AMCase-deficient mice (Fig. 5a). Moreover, as expected, there was no difference in worms recovered from the tissue between the two groups of mice after a primary infection, but impairment of the host immune-mediated worm expulsion in AMCase-deficient mice was strikingly apparent after a secondary infection (Fig. 5b). Wild-type mice had nearly cleared all adult *H. p. bakeri* worms 15 d after reinfection, but AMCase-deficient mice still harbored an average of ~50 worms. Even though the worm burden was not affected by AMCase deficiency during primary infection, the fecundity of the worms differed significantly: *H. p. bakeri* egg output in the AMCase-deficient mice was more than threefold greater than in wild-type animals (Fig. 5c). We observed higher ATP uptake in the worms recovered from AMCase-deficient mice, correlating with the increased fecundity and suggestive of increased worm vitality (Fig. 5d). As with *N. brasiliensis* infection, AMCase-deficient intestines expressed much less *Il13* after both primary and secondary *H. p. bakeri* infections (Fig. 5e). This again corresponded with significantly reduced *Chil3* and *Retnlb* expression in both infections. *Clca1* expression was significantly lower in AMCase-deficient mice, and this was mirrored by the presence of less luminal and cellular mucus in the intestines (Fig. 5f). We ruled out that the immune defect is T cell intrinsic by transferring $CD4^+$ T cells from *H. p. bakeri*–infected wild-type and AMCase-deficient mice into *H. p. bakeri*–infected TCRα-deficient mice. Recipients of cells from both cohorts were equally competent at clearing a primary infection (Supplementary Fig. 4).

Since we found evidence of defective immune priming in AMCase-deficient lungs (Fig. 1f), we hypothesized that immune priming was also deficient in response to GI nematodes. In the duodenum, the type 2 alarmin *Il33* was expressed at similar levels in wild-type and

AMCase-deficient mice in the hours after *H. p. bakeri* worms first reached the proximal intestine (Supplementary Fig. 5). Among the leukocytes in the mesenteric lymph node at this time, however, we found that the percentage and total number of $CD103^+$ $MHCII^+$ $CD11b^+$ dendritic cells were significantly diminished (Fig. 5g). $CD103^+$ DCs have been reported to have a unique capacity to induce gut-homing activity in responding T cells in the mesenteric lymph node[27]. These data show that AMCase has a critical role in initiating type 2 immunity against *H. p. bakeri* in the host GI tract.

DISCUSSION

Collectively, our data indicate that AMCase regulates the early priming of type 2 immune responses in the lung and the GI tract, but that its role in generating protective antinematode immunity in the GI tract is much more critical than its role in the lung. AMCase-deficient and wild-type mice develop similar acute and chronic type 2–driven allergic lung pathology in response to HDM, SEA, or papain inhalation. AMCase ablation also had no effect on the development of type 2-driven granuloma formation around helminth eggs in the lung. In contrast, AMCase is essential for optimal IL-13 production during infection with *N. brasiliensis* and *H. p. bakeri* infection, which is required to activate downstream antiparasite effector molecules (such as Ym1 and Relmβ) and mucus production that cooperatively facilitate parasite expulsion from the intestine.

It is possible that dominance of chitotriosidase in the lung might explain the different outcomes in the lung and gut; chitotriosidase gene expression was largely unaffected by AMCase ablation during allergen challenge but was greatly diminished in intestines of AMCase-deficient mice during *N. brasiliensis* infection. Also, because the stomach exhibits both constitutive and IL-13-inducible AMCase activity, this might serve as the critical location for the initiation of antinematode type 2 immunity as *N. brasiliensis* and *H. p. bakeri* both pass through the stomach on their way to the intestine. Indeed, a prominent role for AMCase in the stomach and duodenum is expected because its chitinolytic activity is greatest at low pH. AMCase functions as a true chitinase in the stomach, as previously suggested[28]; therefore, it is quickly transported into the duodenum, where it may aid in the disruption, release, and/or processing of parasite-associated chitinous antigens that are critical for the initiation of protective type 2 responses in the gut. We found no evidence that the defective type 2 responses observed during nematode infection were T cell intrinsic. Instead, it is likely that the absence of AMCase results in less processing of parasite chitin in the stomach, which would reduce the release of chitin fragments and other antigens that serve as adjuvants for type 2 immunity[8]. This is certainly consistent with the decrease in type 2 immunity and increase in parasite load, fecundity, and worm vitality observed in the infected AMCase-deficient mice. Finding fewer $CD103^+$ DCs in the intestine-draining mesenteric lymph nodes of AMCase-deficient mice also indicates that AMCase stimulates the antiparasite immune response. There is no existing literature suggesting a required role for $CD103^+$ DCs in type 2 responses to parasites[29], but there is evidence they are the major migratory dendritic cell population that presents soluble luminal antigen to T cells[30].

AMCase has long been associated with type 2 cytokine responses that mediate pathogenic allergic inflammation and beneficial immunity to gastrointestinal parasites. The role of

AMCase in these widespread diseases, however, has remained unclear. We show here that AMCase has a critical and nonredundant role in type 2 immune priming during infection with the chitin-containing nematode parasites *N. brasiliensis and H. p. bakeri*. Because AMCase showed a less significant regulatory role in models of allergic lung inflammation and humans lack the machinery to synthesize chitin, it is likely that global exposure to geohelminths rather than airborne allergens provided critical evolutionary pressure to preserve AMCase activity in the human genome.

ONLINE METHODS

Animals

The National Institute of Allergy and Infectious Diseases Division of Intramural Research Animal Care and Use Program, as part of the National Institutes of Health Intramural Research Program, approved all of the experimental procedures (protocol “LPD 16E”). The Program complies with all applicable provisions of the Animal Welfare Act (http://www.aphis.usda.gov/animal_welfare/downloads/awa/awa.pdf) and other federal statutes and regulations relating to animals. AMCase-deficient mice on a C57BL/6N background were kindly provided by L. Fitz and Pfizer. Wild-type C57BL/6N mice, and IL-13-deficient and TCRα-deficient mice on a C57BL/6N background, were obtained from Taconic Farms Inc. Male and female mice between the ages of 6 weeks and 12 weeks were used randomly to begin experimental models because of limited availability, and no sex-specific differences were observed. Groups in individual experiments were sex-matched and age-matched. All animals were housed under specific-pathogen-free conditions at the National Institutes of Health in an American Association for the Accreditation of Laboratory Animal Care–approved facility.

S. mansoni egg–induced lung granuloma model

5,000 *S. mansoni* eggs (Biomedical Research Institute) were injected intraperitoneally on day 0 to sensitize mice. On day 14, mice were challenged again intravenously with 5,000 live eggs containing mature embryos before lungs were harvested on day 18 or 21.

Schistosome egg antigen–induced lung inflammation model

Schistosome egg antigen (SEA) was obtained from sterile LPS-free liver-derived eggs from mice chronically infected with *Schistosoma mansoni*. Mice were intratracheally sensitized and challenged with 10 μg SEA on days 0, 7, 14, 16, and 18. SEA was administered in 30 μl saline to mice anesthetized with isoflurane. Lungs were lavaged and harvested for analysis on day 19.

Acute house dust mite allergen–induced lung inflammation model

Mice were intranasally sensitized with 25 μg of house dust mite (HDM, Greer) or PBS on days 0, 1, and 2. On days 15, 16, 17, and 18, mice were intranasally challenged with 5 μg of HDM or PBS. HDM was administered in 30 μl PBS to mice anesthetized with isoflurane. Lungs were lavaged and harvested for analysis on day 19.

Chronic house dust mite allergen–induced lung inflammation model

Mice were intranasally sensitized with 25 μg of house dust mite (HDM, Greer) or PBS on days 0, 1, and 2. On days 14, 15, 16, 28, 29, 30, 42, 43, and 44, mice were intranasally challenged with 5 μg of HDM or PBS. Lungs were lavaged and harvested for analysis on day 45.

Acute papain-induced lung inflammation model

Mice were intranasally sensitized with 12.5 μg of papain (*Carica papaya*, EMD Millipore) or water on days 0, 1, and 2. On days 15, 16, 17, and 18, mice were intranasally challenged with 10 μg of papain or PBS. Papain was administered in 30 μl PBS to mice anesthetized with isoflurane. Lungs were lavaged and harvested for analysis on day 19.

Nippostrongylus brasiliensis infection

Third-stage (L3) larvae were prepared as described previously[31], and 500 were injected subcutaneously into the nape of the neck of each mouse. Feces were collected on days 6–10 post-infection for egg counts. Adult worms were counted in the small intestine on days 5, 8, 10, or 14. Representative sections of lung and small intestinal tissue were taken for histology and qPCR analysis on day 8.

Heligmosomoides polygyrus bakeri infection

As described previously[32], mice were inoculated perorally with 200 L3, and 2 weeks later, worms were expelled by administering 1–2 mg pyrantel pamoate. 4 weeks later, the sensitized mice were challenged with *H. p. bakeri* (secondary) while naive mice were inoculated with 200 L3 for the first time as controls (primary). 12 d after this, mice were sacrificed for analysis. Eggs were counted in the feces, and tissue was collected for histology and gene expression assay by qPCR. Adult worms were counted in the intestines 15 d after primary inoculation and secondary challenge. The ATPLite Luminescence Assay System (PerkinElmer) was used to measure ATP content of adult worms collected from the intestines of primary infected mice. For some experiments, the proximal small intestine and mesenteric lymph nodes were harvested 3.5 d post-infection for studies of the innate immune response.

T cell transfer

Wild type and AMCase-deficient mice were subjected to primary *H. p. bakeri* infection with 200 L3. Two weeks later, mesenteric lymph nodes were harvested and ground into a single cell suspension through a 70 μm filter on ice. $CD4^+$ T cells were isolated from the leukocytes using Dynabeads Untouched Mouse CD4 Cells kit (Invitrogen). TCRα-deficient mice were infected with *H. p. bakeri* and on the same day were injected intravenously with 2×10^5 T cells from wild-type mice, 2×10^5 T cells from AMCase-deficient mice, or no T cells. *H. p. bakeri* adult worms were counted from the recipient mice 15 d later.

Bronchoalveolar lavage

1 ml of ice-cold PBS supplemented with 5 mM EDTA was injected through the trachea into the lungs and aspirated using a syringe.

Histopathology

Representative samples of lung or intestinal tissue were fixed in Bouin-Hollande solution, embedded in paraffin for sectioning, and stained (Histopath of America) with Wright's Giemsa to measure eosinophil accumulation, hematoxylin and eosin to analyze inflammation, picrosirius red to analyze fibrosis, or periodic acid–Schiff (PAS) stain for analysis of mucus production. A blinded pathologist averaged two diameters of approximately 30 granulomas with an ocular micrometer and the volume of each granuloma was calculated assuming a spherical shape. Granulomatous eosinophils were quantified in the same Giemsa-stained sections. The blinded pathologist also scored additional stained sections for fibrosis and mucus production. Images were scanned at 40× with an Aperio ScanScope (Leica Biosystems).

Immunofluorescence staining and microscopy

Immunodetection of AMCase was performed on lung and intestinal tissue sections with rabbit sera immunized against recombinant murine AMCase that was a gift from MedImmune. MedImmune validated the antisera in-house for use in mice.

Leukocyte isolation from lung tissue for analysis by flow cytometry

About 200 mg of lung tissue was ground into a single-cell suspension through a 100-μm nylon mesh. Leukocytes were separated on a 40% Percoll (Sigma-Aldrich) gradient (2,000 r.p.m. for 15 min) and treated for 2 min with 1 ml ACK (ammonium chloride–potassium bicarbonate) lysis buffer to lyse erythrocytes. After 3 h of stimulation with phorbol 12-myristate13-acetate (PMA, 10 ng/ml), ionomycin (1 μg/ml), and Brefeldin A (BFA, 10 μg/ml), leukocytes were fixed and permeabilized for 30 min (Cytofix/Cytoperm buffer; BD Biosciences) and then stained for 30 min with antibodies to CD4 (1:200 dilution; RM4-5; eBioscience), IL-4 (1:200 dilution; 11B11; eBioscience), IL-5 (1:200 dilution; TRFK5; BD Pharmingen), and IL-13 (1:200 dilution; eBio13A; eBioscience) diluted in the Permwash buffer (BD Biosciences). Unstimulated lung leukocyte aliquots were set aside and stained for 30 min with anti-SiglecF (1:200 dilution; E50-2440; BD Biosciences). Positive SiglecF staining and scatter profiling were used to identify eosinophils by flow cytometry. Expression of CD4, SiglecF, and the intracellular cytokines was analyzed with a BD FACSCanto II flow cytometer and FlowJo v.7.6 software (Tree Star). For some experiments, leukocytes were isolated as above approximately 12 h after the last of three sensitization doses of house dust mite. Some cells were stimulated as described above, washed with Hank's Balanced Salt Solution, and stained with Live/Dead Fixable Blue (Life Technologies), anti-CD16/32 (1:500 dilution; BioLegend), and a biotin-conjugated lineage cocktail (1:100 dilution; eBioscience) composed of antibodies against CD8 (eBioH35-17.2), CD11b (M1/70), CD19 (MB19-1), CD49b (DX5), Gr-1 (RB6-8C5), NK1.1 (PK136), γδTCR (eBioGL3), TER-119, and CD11c (N418) for 20 min at 4 °C. Next, cells were washed with FACS buffer and stained with a streptavidin-conjugated antibody and antibodies against CD16/32, Thy1.2 (1:400 dilution; 53–2.1; BioLegend), CD45 (1:400 dilution; 30-F11; BioLegend), and TCRβ (1:200 dilution; H57-597; eBioscience) for 30 min at 4 °C. The cells were washed again with FACS buffer before being fixed with 2% paraformaldehyde for 15 min at room temperature. Cells were then permeabilized by

washing with 0.5% saponin (Sigma) and stained with antibodies for CD4 (1:500 dilution; RM4-5; BDBiosciences), IL5 (1:200 dilution), IL13 (1:100 dilution), and CD16/32 (1:500 dilution) in the same buffer for 45 min at 4 °C. The cells were again washed in 0.5% saponin before being resuspended in FACS buffer for analysis with a BD LSRFortessa flow cytometer. Type 2 innate lymphoid cells were identified as live Lin^- $TCR\beta^-$ $CD4^-$ $Thy1.2^+$ $CD45^+$ $IL\text{-}5^+$ $IL\text{-}13^+$. Some cells were left unstimulated for measurement of Gata3 expression. These cells were processed as above until they were permeabilized with Fixation/Permeabilization solution (eBioscience) and then stained with antibodies against CD4 (1:400 dilution; RM4-5; BioLegend) and Gata3 (1:40 dilution; L50-823; BDBiosciences) and washed with permeabilization buffer (eBioscience). $Gata3^+$ innate lymphoid cells were also identified with a BD LSRFortessa. All antibodies are commercially available, and validation profiles and references are available on corresponding commercial websites.

Leukocyte isolation from mesenteric lymph nodes for dendritic cell identification

3.5 d post-infection with *H. p. bakeri*, mesenteric lymph nodes were ground into a single-cell suspension through a 70-μm cell strainer on ice. Leukocytes were fixed and then stained for 30 min with antibodies for CD16/32 (1:100 dilution; BD Biosciences), CD45 (1:200 dilution; 30-F11; BioLegend), Ly6G (1:400 dilution; 1A8; BD Pharmingen), CD11c (1:200 dilution; 3.9; BioLegend), MHCII 1Ab (1:200 dilution; M5/114.15.2; eBioscience), CD11b (1:200 dilution; M1/70; BioLegend), and CD103 (1:200 dilution; M290; BDBiosciences). $CD45^+$ $Ly6G^-$ $CD11c^+$ $MHCII^+$ $CD11b^+$ $CD103^+$ cells were identified with a BD LSRFortessa and FlowJo v.7.6 software. All antibodies are commercially available, and validation profiles and references are available on corresponding commercial websites.

RNA isolation and quantitative real-time PCR

Lung, stomach, or intestinal tissue was homogenized in TRIzol Reagent (Life Technologies) using Precellys 24 (Bertin Technologies). Total RNA was extracted from the homogenate by addition of chloroform followed by the recommendations of the MagMax-96 Total RNA Isolation Kit (Life Technologies). RNA was then reverse transcribed using SuperScript II Reverse Transcriptase (Life Technologies). Real-time RT-PCR was performed on an ABI Prism 7900HT Sequence Detection System (Applied Biosystems). Quantities of mRNA expressed by a particular gene were determined using Power SYBR Green PCR Master Mix (Applied Biosystems), normalized to ribosomal protein, large, P2 (RPLP2) mRNA levels in each sample, and then articulated as a relative increase or decrease compared with mRNA levels expressed by the same gene in naive controls. We used the following primer sequences: *Rplp2*: forward 5′-TACGTCGCCTCTTACCTGCT-3′, reverse 5′-GACCTTGTTGAGCCGATCAT-3′; *Chia1*: forward 5′-TGGACCTGGACTGGGAATACC-3′, reverse 5′-TGGGCCTGTTGCTCTCAATAG-3′; *Il4*: forward 5′-ACGAGGTCACAGGAGAAGGGA-3′, reverse 5′-AGCCCTACAGACGAGCTCACTC-3′; *Il13*: forward 5′-CCTCTGACCCTTAAGGAGCTTAT-3′, reverse 5′-CGTTGCACAGGGGAGTCT-3′; *Chil3*: forward 5′-CATGAGCAAGACTTGCGTGAC-3′, reverse 5′-GGTCCAAACTTCCATCCTCCA-3′; *Relnlb*: forward 5′-CGTCTCCCTTTTCCCACTG-3′, reverse 5′-CAGGAGATCGTCTTAGGCTCTT-3′; *Retnla*: forward 5′-

CCCTCCACTGTAACGAAGACTC-3′, reverse 5′-CACACCCAGTAGCAGTCATCC-3′; *Clca1*: forward 5′-AGGAAAACCCCAAGCAGTG-3′, reverse 5′-GCACCGACGAACTTGATTTT-3′; *Il5*: forward 5′-TGACAAGCAATGAGACGATGAGG-3′, reverse 5′-ACCCCCACGGACAGTTTGATTC-3′; *Il33*: forward 5′-CACATTGAGCATCCAAGGAA-3′, reverse 5′-AACAGATTGGTCATTGTATGTACTCAG-3′; *Tslp*: forward 5′-ACGGATGGGGCTAACTTACAA-3′, reverse 5′-AGTCCTCGATTTGCTCGAACT-3′; *Il25*: forward 5′-ACAGGGACTTGAATCGGGTC-3′, reverse 5′-TGGTAAAGTGGGACGGAGTTG-3′; *Mrc1*: forward 5′-CCCAAGGGCTCTTCTAAAGCA-3′, reverse 5′-CGCCGGCACCTATCACA-3′; *Chit1*: forward 5′-TGGGCAGGTGTGATGACTCT-3′, reverse 5′-CCCTGGGAAAGAACCGAACTG-3′.

Statistical analysis

All data were analyzed with Prism (Version 5; GraphPad). Data sets were compared with a two-tailed *t*-test, and differences were considered significant if P values were <0.05. No statistical methods were used to predetermine sample size. Group sample size was chosen using records of variance in past experiments, and variance is similar between groups being statistically compared. Mice or samples were randomly assigned to experimental groups or processing orders. Group allocation was blinded for all mouse work, when possible (for example, administration of allergens and infectious agents, sample quantification and analysis, pathology scoring). Samples or data points were excluded only in the case of a technical equipment or human error that caused a sample to be poorly controlled for.

Supplementary Material

Refer to Web version on PubMed Central for supplementary material.

Acknowledgments

This research was supported by the Intramural Research Program of the National Institutes of Health, National Institute of Allergy and Infectious Disease. The funders had no role in study design, data collection and analysis, decision to publish, or preparation of the manuscript. We thank MedImmune for generating the anti-AMCase rabbit sera, C. Mainhart for genotyping, T. Gieseck and K. Kindrachuk for discussions, and the animal care staffs of Buildings 50 and 14BS at the US National Institutes of Health's Bethesda, Maryland campus for the conscientious care of mice.

References

1. Lenardon MD, Munro CA, Gow NA. Chitin synthesis and fungal pathogenesis. Curr. Opin. Microbiol. 2010; 13:416–423. [PubMed: 20561815]
2. Neville AC, Parry DA, Woodhead-Galloway J. The chitin crystallite in arthropod cuticle. J. Cell. Sci. 1976; 21:73–82. [PubMed: 932111]
3. Veronico P, et al. Nematode chitin synthases: gene structure, expression and function in *Caenorhabditis elegans* and the plant parasitic nematode *Meloidogyne artiellia*. Mol. Genet. Genomics. 2001; 266:28–34. [PubMed: 11589574]
4. Foster JM, Zhang Y, Kumar S, Carlow CK. Parasitic nematodes have two distinct chitin synthases. Mol. Biochem. Parasitol. 2005; 142:126–132. [PubMed: 15869814]

5. Boot RG, et al. Identification of a novel acidic mammalian chitinase distinct from chitotriosidase. J. Biol. Chem. 2001; 276:6770–6778. [PubMed: 11085997]
6. Renkema GH, Boot RG, Muijsers AO, Donker-Koopman WE, Aerts JM. Purification and characterization of human chitotriosidase, a novel member of the chitinase family of proteins. J. Biol. Chem. 1995; 270:2198–2202. [PubMed: 7836450]
7. Zhu Z, et al. Acidic mammalian chitinase in asthmatic Th2 inflammation and IL-13 pathway activation. Science. 2004; 304:1678–1682. [PubMed: 15192232]
8. Reese TA, et al. Chitin induces accumulation in tissue of innate immune cells associated with allergy. Nature. 2007; 447:92–96. [PubMed: 17450126]
9. Ramanathan M Jr, Lee WK, Lane AP. Increased expression of acidic mammalian chitinase in chronic rhinosinusitis with nasal polyps. Am. J. Rhinol. 2006; 20:330–335. [PubMed: 16871939]
10. Fitz LJ, et al. Acidic mammalian chitinase is not a critical target for allergic airway disease. Am. J. Respir. Cell. Mol. Biol. 2012; 46:71–79. [PubMed: 21836154]
11. Kim LK, et al. AMCase is a crucial regulator of type 2 immune responses to inhaled house dust mites. Proc. Natl. Acad. Sci. USA. 2015; 112:E2891–E2899. [PubMed: 26038565]
12. Wynn TA. Type 2 cytokines: mechanisms and therapeutic strategies. Nat. Rev. Immunol. 2015; 15:271–282. [PubMed: 25882242]
13. Nair MG, et al. Chitinase and Fizz family members are a generalized feature of nematode infection with selective upregulation of Ym1 and Fizz1 by antigen-presenting cells. Infect. Immun. 2005; 73:385–394. [PubMed: 15618176]
14. Yagi R, et al. The transcription factor GATA3 is critical for the development of all IL-7Rα-expressing innate lymphoid cells. Immunity. 2014; 40:378–388. [PubMed: 24631153]
15. Bierbaum S, et al. Polymorphisms and haplotypes of acid mammalian chitinase are associated with bronchial asthma. Am. J. Respir. Crit. Care. Med. 2005; 172:1505–1509. [PubMed: 16179638]
16. Wiesner DL, et al. Chitin recognition via chitotriosidase promotes pathologic type-2 helper T cell responses to cryptococcal infection. PLoS Pathog. 2015; 11:e1004701. [PubMed: 25764512]
17. Seibold MA, et al. Chitotriosidase is the primary active chitinase in the human lung and is modulated by genotype and smoking habit. J. Allergy Clin. Immunol. 2008; 122:944–950. [PubMed: 18845328]
18. Sandler NG, Mentink-Kane MM, Cheever AW, Wynn TA. Global gene expression profiles during acute pathogen-induced pulmonary inflammation reveal divergent roles for Th1 and Th2 responses in tissue repair. J. Immunol. 2003; 171:3655–3667. [PubMed: 14500663]
19. Albonico M, et al. Controlling soil-transmitted helminthiasis in pre-school-age children through preventive chemotherapy. PLoS Negl. Trop. Dis. 2008; 2:e126. [PubMed: 18365031]
20. Zaph C, Cooper PJ, Harris NL. Mucosal immune responses following intestinal nematode infection. Parasite Immunol. 2014; 36:439–452. [PubMed: 25201407]
21. Herbert DR, et al. Intestinal epithelial cell secretion of RELM-beta protects against gastrointestinal worm infection. J. Exp. Med. 2009; 206:2947–2957. [PubMed: 19995957]
22. Sutherland TE, et al. Chitinase-like proteins promote IL-17-mediated neutrophilia in a tradeoff between nematode killing and host damage. Nat. Immunol. 2014; 15:1116–1125. [PubMed: 25326751]
23. Sabo-Attwood T, et al. Gene expression profiles reveal increased mClca3 (Gob5) expression and mucin production in a murine model of asbestos-induced fibrogenesis. Am. J. Pathol. 2005; 167:1243–1256. [PubMed: 16251409]
24. Hasnain SZ, et al. Muc5ac: a critical component mediating the rejection of enteric nematodes. J. Exp. Med. 2011; 208:893–900. [PubMed: 21502330]
25. McKenzie GJ, Fallon PG, Emson CL, Grencis RK, McKenzie AN. Simultaneous disruption of interleukin (IL)-4 and IL-13 defines individual roles in T helper cell type 2-mediated responses. J. Exp. Med. 1999; 189:1565–1572. [PubMed: 10330435]
26. Urban JF Jr, et al. IL-13, IL-4Rα, and Stat6 are required for the expulsion of the gastrointestinal nematode parasite *Nippostrongylus brasiliensis*. Immunity. 1998; 8:255–264. [PubMed: 9492006]

27. Johansson-Lindbom B, et al. Functional specialization of gut CD103^{+} dendritic cells in the regulation of tissue-selective T cell homing. J. Exp. Med. 2005; 202:1063–1073. [PubMed: 16216890]

28. Strobel S, Roswag A, Becker NI, Trenczek TE, Encarnação JA. Insectivorous bats digest chitin in the stomach using acidic mammalian chitinase. PLoS One. 2013; 8:e72770. [PubMed: 24019876]

29. Iwasaki A, Medzhitov R. Control of adaptive immunity by the innate immune system. Nat. Immunol. 2015; 16:343–353. [PubMed: 25789684]

30. Jaensson E, et al. Small intestinal CD103^{+} dendritic cells display unique functional properties that are conserved between mice and humans. J. Exp. Med. 2008; 205:2139–2149. [PubMed: 18710932]

References

31. Katona IM, Urban JF Jr, Scher I, Kanellopoulos-Langevin C, Finkelman FD. Induction of an IgE response in mice by *Nippostrongylus brasiliensis*: characterization of lymphoid cells with intracytoplasmic or surface IgE. J. Immunol. 1983; 130:350–356. [PubMed: 6600186]

32. Liu Q, et al. B cells have distinct roles in host protection against different nematode parasites. J. Immunol. 2010; 184:5213–5223. [PubMed: 20357259]

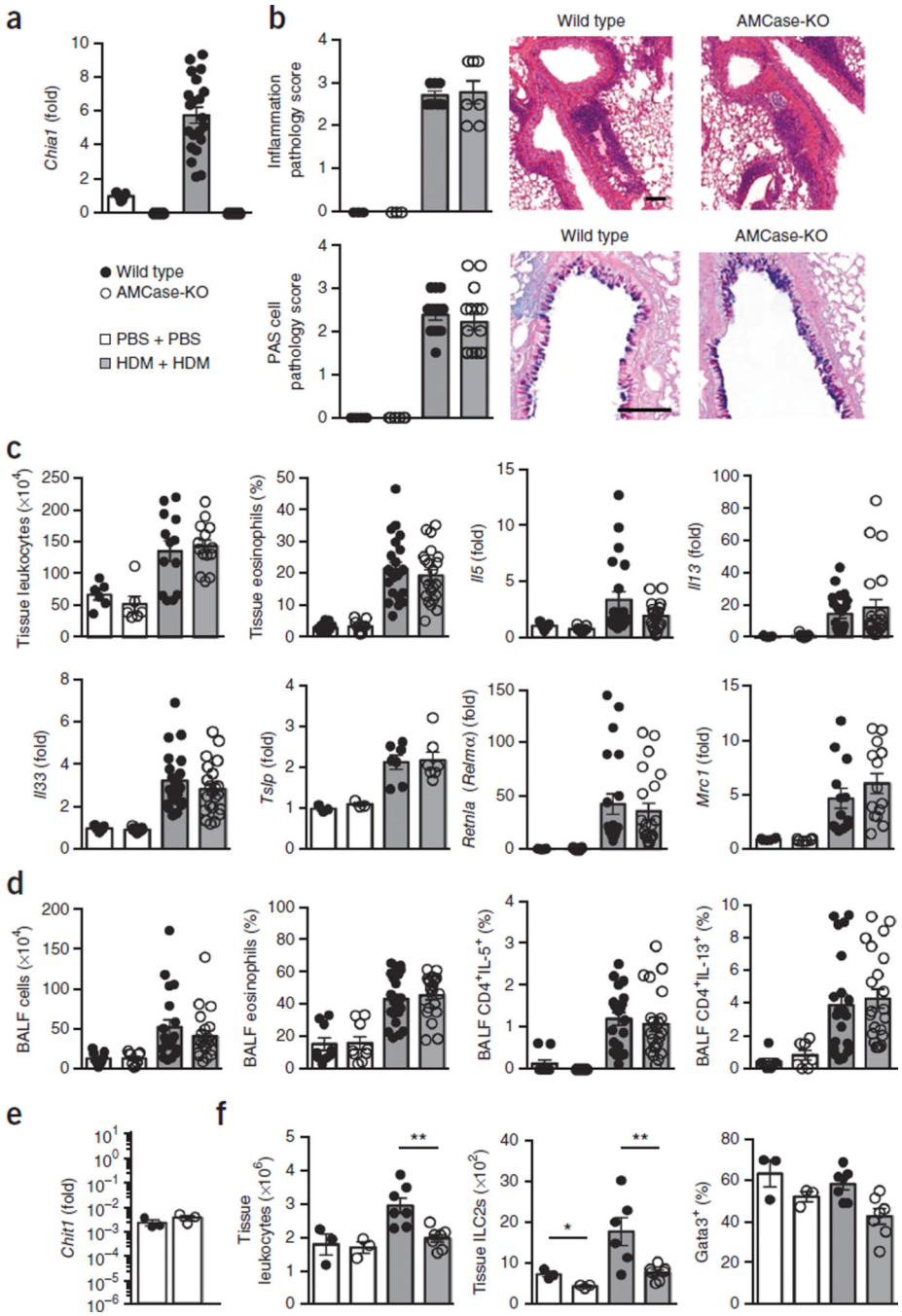

Figure 1.

AMCase-deficient mice develop acute HDM-induced lung allergy despite diminished ILC2s. (**a**) Quantitative PCR analysis of AMCase (*Chia1*) gene expression in lung tissue from wild-type or AMCase-deficient mice (AMCase-KO) sensitized and challenged intranasally with PBS ($n = 9$ mice per genotype) or house dust mite (HDM) ($n = 21$ mice per genotype), expressed as fold change relative to expression of PBS-treated wild-type mice. (**b**) Lung pathology of mice in **a**. At left, scores (scale 0–4, with 4 being the worst) of tissue sections stained with hematoxylin and eosin (inflammation; PBS, $n = 3$; HDM, $n = 7$) and periodic

acid-Schiff (PAS; PBS, $n = 6$; HDM, $n = 15$; pooled from two experiments). At right, representative staining (scale bars, 100 μm). (**c**) Lung tissue leukocyte (PBS: $n = 6$, HDM: $n = 15$ pooled from two experiments) and eosinophil quantification (PBS: $n = 9$, HDM: $n = 22$; pooled from three experiments) from three lung lobes of mice in **a** and gene expression analysis (PBS: $n = 9$, HDM: $n = 22$; pooled from three experiments). (**d**) Leukocyte and eosinophil quantification and intracellular cytokine analysis of lymphocytes collected from bronchoalveolar lavage fluid (BALF) of mice in **a** (PBS, $n = 9$; HDM, $n = 22$). (**e**) Chitotriosidase gene expression in lung tissue (representative of naive and allergic lungs) (wild type, $n = 3$; AMCase-KO, $n = 3$) shown relative to expression of the housekeeping gene *Rplp2*. (**f**) Following only sensitization of wild-type or AMCase-KO mice with intranasal PBS ($n = 3$) or HDM ($n = 7$), quantification of total lung leukocytes, total lung IL-4+IL-13+ ILC2s, and Gata3+ cells among ILCs in the lung. Data are pooled from three experiments (**a**,**d**) or are from one experiment representative of three independent experiments with similar results (**e,f**). Error bars, s.e.m.; each data point represents a value for an individual mouse.

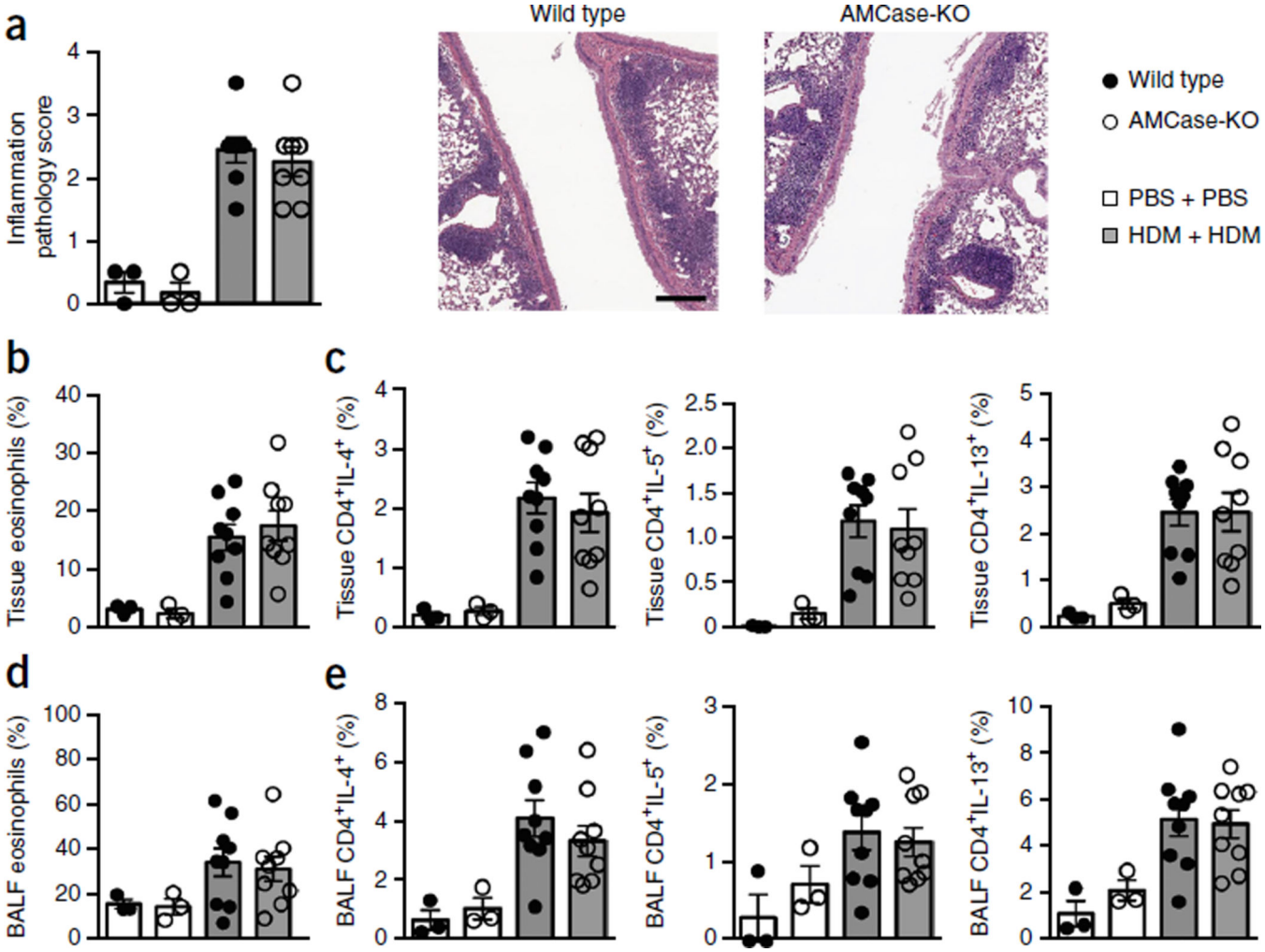

Figure 2.

Chronic HDM induces similar allergy in the lungs of wild-type and AMCase-deficient mice. (**a**) Histopathology scoring and representative sections stained with H&E (scale bar, 200 μm) from wild-type or AMCase-deficient (AMCase-KO) mice sensitized and challenged intranasally with PBS (n = 3 mice per genotype) or house dust mite (HDM) (n = 8 mice per genotype) for 45 d. (**b**) Quantification of eosinophils in the lung tissue of mice in **a** (PBS, n = 3; HDM, n = 9). (**c**) Intracellular cytokine analysis of lung tissue lymphocytes of mice in **a** (PBS, n = 3; HDM, n = 9). (**d**) Quantification of eosinophils in BALF of mice in **a** (PBS, n = 3; HDM, n = 9). (**e**) Intracellular cytokine analysis of BALF lymphocytes of mice in **a** (PBS, n = 3; HDM, n = 9). Data are pooled from two experiments with similar results. Error bars, s.e.m.; each data point represents a value for an individual mouse.

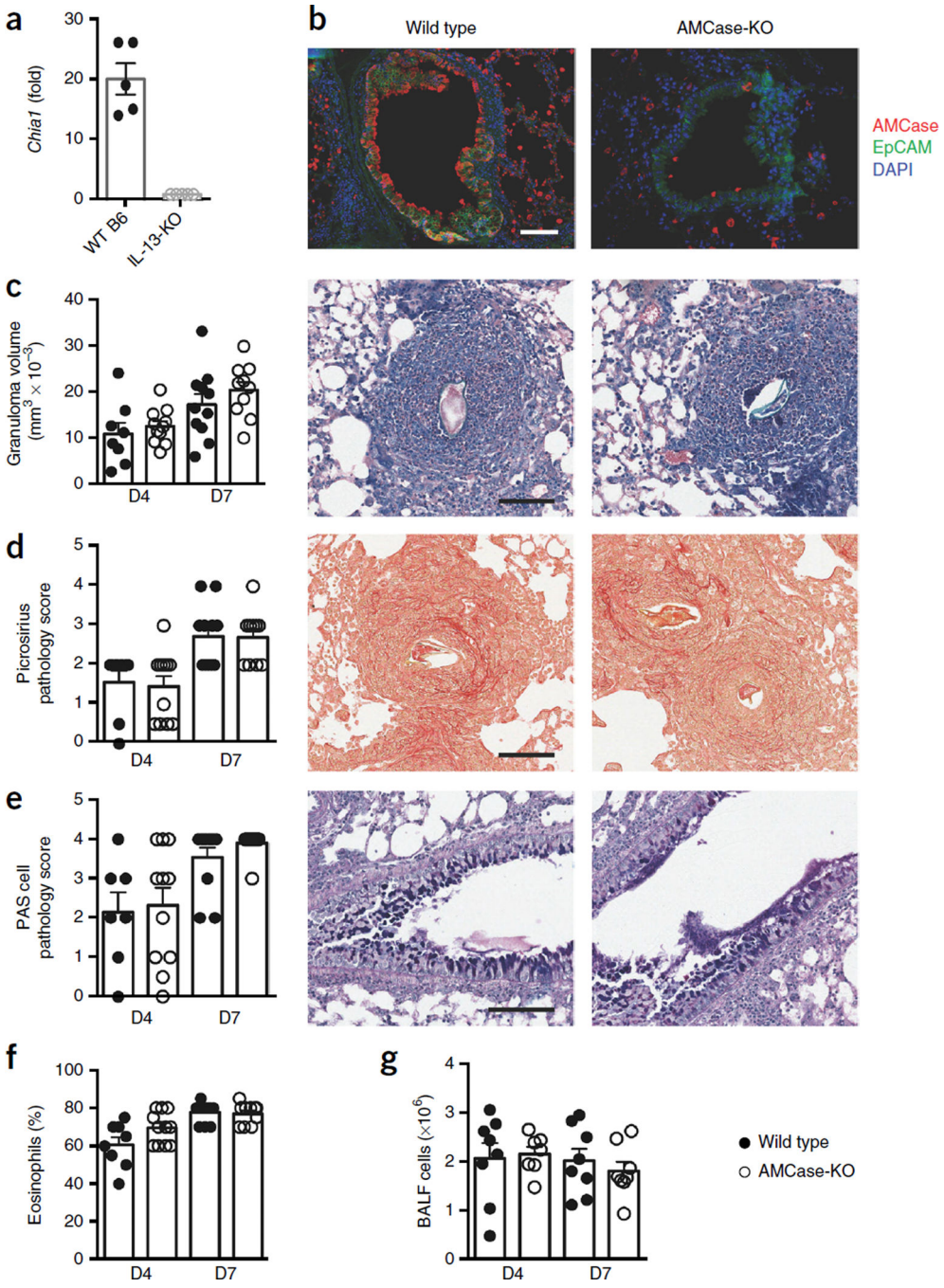

Figure 3.

AMCase-deficient mice develop *S. mansoni* egg–induced lung granulomas. (**a**) Quantitative PCR analysis of *Chia1* expression in lung tissue from wild-type ($n = 5$) or IL-13-deficient mice (IL-13-KO) ($n = 5$) 7 d after intravenous injection of *S. mansoni* eggs. (**b**) Immunofluorescence of lung airway sections 7 d after intravenous egg injection. (**c**) Granulomatous lung pathology as measured using Giemsa stain 4 or 7 d after intravenous egg injection into wild-type (day 4 (D4), $n = 8$; day 7 (D7), $n = 11$) or AMCase-KO mice (day 4, $n = 11$; day 7, $n = 10$). (**d**) Lung sections from mice in **c** scored for fibrosis by

picrosirius stain. (**e**) Lung sections from mice in **c** scored for mucus in goblet cells by PAS stain. (**f**) Quantification of eosinophils comprising granulomas from Giemsa-stained lung sections of mice in **c**. (**g**) Quantification of BALF cells from mice in **c**. Scale bars: 50 μm (**b**), 100 μm (**c**–**e**). Data are representative of two experiments with similar results. Error bars, s.e.m.; each data point represents a value for an individual mouse.

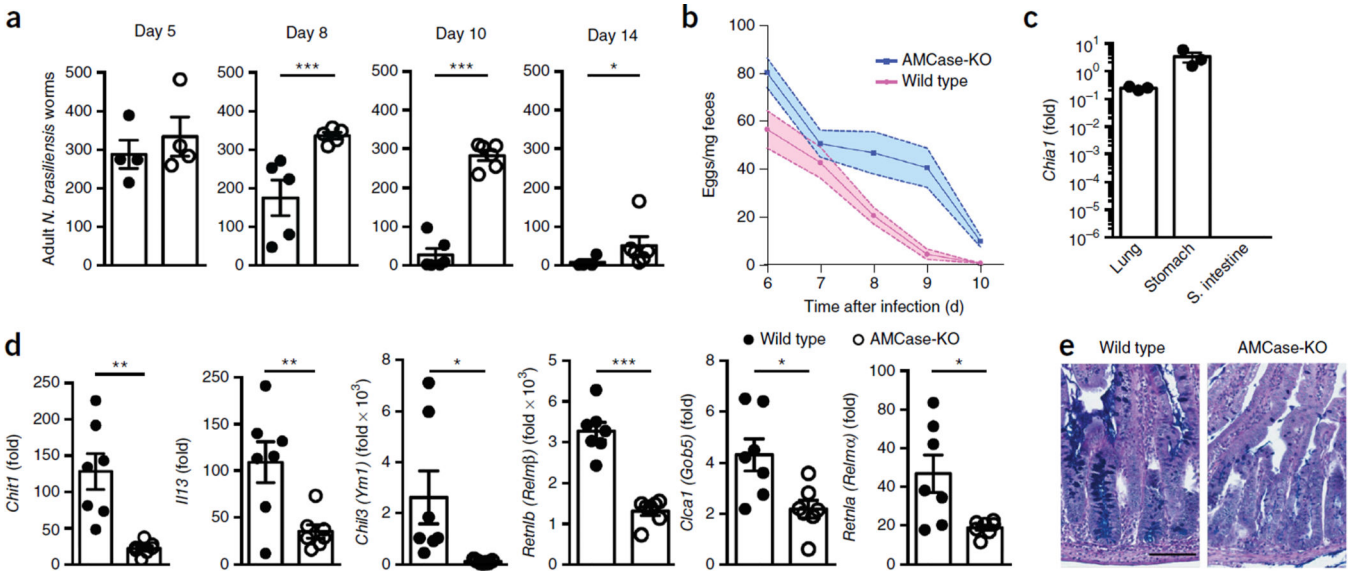

Figure 4.

AMCase is critical for type 2–mediated protection against *N. brasiliensis*. (**a**) Quantification of nematodes from intestines of wild-type or AMCase-deficient (AMCase-KO) mice ($n = 5$ per genotype per time point) on the days after infection indicated. (**b**) Fecal egg counts (day 6, $n = 14$ mice per genotype; day 7, $n = 14$ per genotype; day 8, $n = 13$ per genotype; day 9, $n = 8$ per genotype; day 10, $n = 8$ per genotype). (**c**) Quantitative PCR analysis of *Chia1* expression in tissues from naive wild-type mice ($n = 3$) shown as fold values relative to expression of the housekeeping gene *Rplp2*. (**d**) Quantitative PCR analysis of gene expression in small intestinal tissue of wild-type ($n = 7$) or AMCase-KO mice ($n = 7$) 8 d after *N. brasiliensis* infection, shown relative to expression in naive mice. (**e**) Representative PAS staining from small intestinal sections from mice in **d** (scale bar, 100 μm). $^{*}P < 0.05$, $^{**}P < 0.01$, $^{***}P < 0.001$ (Student's *t*-test). Data are representative of two experiments with similar results. Error bars, s.e.m.; each data point represents a value for an individual mouse.

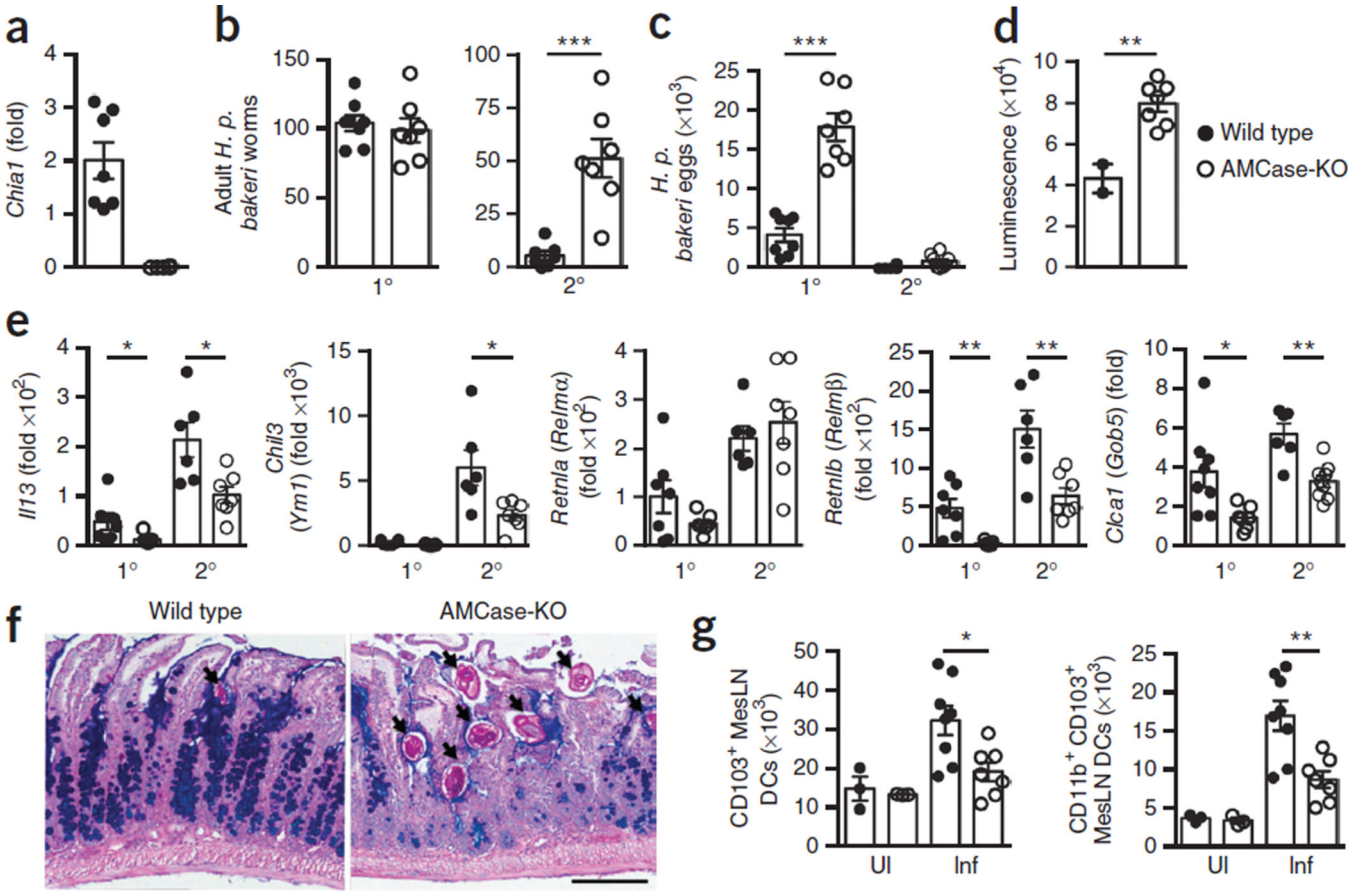

Figure 5.

Type 2 immunity against *H. p. bakeri* is impaired in AMCase-deficient mice. (**a**) Quantitative PCR analysis of *Chia1* expression in stomach tissue from wild-type ($n = 7$) or AMCase-deficient (AMCase-KO) mice ($n = 6$) 15 d after primary infection with *H. p. bakeri*, expressed as fold change relative to expression in stomach tissue from naive wild-type mice ($n = 3$). (**b**) Adult worm burden in the intestines 15 d after primary (1°) or secondary (2°) challenge of wild-type ($n = 8$) or AMCase-KO mice ($n = 7$). (**c**) Fecal egg counts 12 d after primary or secondary challenge of wild-type ($n = 8$) or AMCase-KO mice ($n = 7$). (**d**) Adult worm ATP levels quantified by light produced by the reaction of ATP with added luciferase 12 d after primary challenge of wild-type ($n = 2$) or AMCase-KO mice ($n = 7$). (**e**) Quantitative PCR analysis of gene expression in small intestinal tissue of wild-type ($n = 7$) or AMCase-KO mice ($n = 7$) 12 d after infection, shown relative to expression in naive mice. (**f**) PAS staining of representative small intestinal tissue sections 12 d after secondary challenge (scale bar, 200 μm; arrows indicate parasites). (**g**) Quantification of mesenteric lymph node dendritic cells from wild-type ($n = 8$) or AMCase-KO mice ($n = 7$) 3.5 d after infection (Inf) or from uninfected (UI) wild-type or AMCase-KO mice ($n = 3$ per genotype). $^{*}P < 0.05$, $^{**}P < 0.01$, $^{***}P < 0.001$ (Student's *t*-test). Data are representative of two experiments with similar results. Error bars, s.e.m.; each data point represents a value for an individual mouse.